

# SOC and diffusion rate estimation in redox flow batteries: An I&I-based high-gain observer approach

Alejandro Clemente, Andreu Cecilia and Ramon Costa-Castelló

**Abstract**—This paper presents an adaptive non-linear observer for the state of charge estimation in vanadium redox flow batteries. The study is based directly on the use of non-linear equations that describe the evolution of the species concentration inside the system, and a nonlinear cell voltage expression that takes into account the effect of overpotentials. Moreover, a more realistic approach is used which does not consider that the electrolyte concentration is the same in the catholyte and anolyte sides of the system. It is shown that the state of charge can be estimated through the measurement of the output voltage and a high-gain observer. Nonetheless, the accuracy of the estimation is affected by uncertainty in the system diffusion rates. For this reason, the observer is robustified by means of an immersive and invariance adaptive parameter estimation. The results are validated in a numerical simulation.

## I. INTRODUCTION

The role of the renewable energy has grown during the last years, and it will continue expanding. The International Energy Agency (IEA) has estimated that in the next five years the total renewable energy capacity will expand by 50% [1]. In particular, growth can be seen in the creation of wind and solar plants. Due to their intermittent nature, the development of large-scale energy storage as a support tool for these plants has become one of its main challenges. Is in this field, where redox flow batteries (RFB) have become a promising solution [2].

A RFB is an electrochemical energy storage system that uses four chemical species divided in two identical subsystems called anolyte and catholyte. The system is composed by two parts. On the one hand, an electrochemical cell where redox reactions take place in order to generate a certain load current during a charging or discharging process. On the other hand, a set of tanks where energy is stored in the form of electrolyte. Both tanks and cells are connected through pipes, and by means of pumps the electrolyte can flow through the system. A general scheme of a RFB is depicted in Fig. 1. Among the different types of RFB, all-vanadium redox flow batteries (VRFB) have become the best choice due to the fact that all species are vanadium oxides [3]. A VRFB is completely composed by vanadium species

This research was funded by the CSIC under the PTI FLOWBAT 2021 project (ref. 642 201980E101), the Spanish Ministry of Economy and Competitiveness under Project DOVELAR (ref. RTI2018-096001-B-C32), and by the Spanish State Research Agency through the María de Maeztu Seal of Excellence to IRI (MDM-2016-0656).

A. Clemente, A. Cecilia and R. Costa-Castelló are with the Institut de Robòtica i Informàtica Industrial, CSIC-UPC Llorens i Artigas 4-6, 08028 Barcelona, Spain (e-mail: alejandro.clemente.leon@upc.edu and andreu.cecilia@upc.edu and ramon.costa@upc.edu). (Corresponding author: Alejandro Clemente)

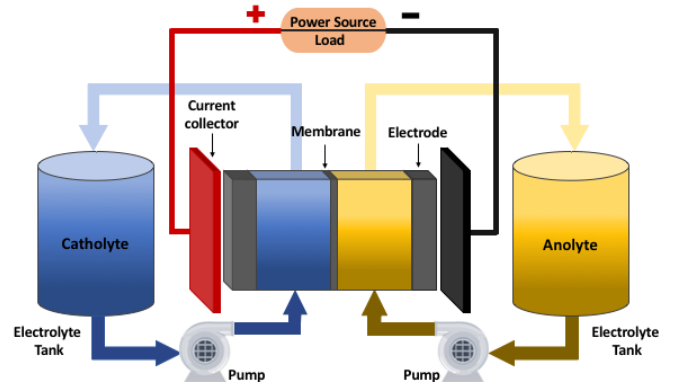


Fig. 1. Scheme of a redox flow battery.

in four different oxidation states. The anolyte is composed by species  $V^{2+}$  and  $V^{3+}$ , while the catholyte is made up of the species  $V^{4+}$  and  $V^{5+}$ .

Within the analysis and study of RFB systems, one of the most important challenges has become the determination of the state of charge (SOC). This variable indicates how much energy is stored in the system and is crucial for its adequate operation [4]. In VRFB, the SOC can be directly computed by means of the concentration of species inside the tanks. In the literature, one can find multiple techniques to estimate the tank's concentration [5]. For example, through the use of color, density or conductivity analysis [6]. However, such techniques are too slow, intrusive and inaccurate to be a valid option for RFB real-time control. Taking into account the impossibility to obtain an adequate measure of the SOC, some studies propose an observer to estimate its value.

The most common measure used to estimate the SOC is the open circuit voltage (OCV) which is the potential difference in the cell. Skyllas-Kazacos, who was a pioneer in the use of vanadium redox flow batteries (VRFB), developed an Extended Kalman Filter (EKF) method to estimate the SOC measuring the OCV and assuming that the concentration of vanadium species in both cell and stack are the same [7]. Following studies used the EKF to estimate the SOC by means of an electric model [8], or thermal-dependant ones [9]. However, the EKF is based on linearizing the RFB's model, which results in a local solution of the estimation problem and may present robustness issues to high nonlinearities. For this reason, some authors studied the implementation of nonlinear observers. Specifically, a sliding mode observer (SMO) have been used for the presented purpose [10], being especially useful for dealing with nonlinear models.

Another concern in the SOC estimation is the parametric uncertainty, which deteriorates the observer's accuracy. Con-

sequently, some authors studied the use of adaptive estimation techniques to reduce the effect of said uncertainty[11]. Unfortunately, available adaptive techniques are commonly implemented through recursive least squares methods. Therefore, state and parameter estimation convergence can only be proved through the persistence excitation condition[11].

This paper presents a nonlinear high-gain observer [12] that can estimate the *SOC* of a VRFB, dealing directly with the nonlinear electrochemical model. This work implements a model that describes the behaviour of the different vanadium species in both cell and tanks. Moreover, differing from other studies, it has been considered a distinction between the flow rates in both parts of the system, as well as the total vanadium concentration. This leads to a more realistic model of the real system. Regarding the OCV, the model uses a more realistic approximation from the Nerst equation that takes into account not only the species, but also the proton concentration, as well as the overpotential effect, which improves the estimation accuracy. Moreover, it is assumed that the species diffusion rates are unknown. For this reason, the observer is coupled with an adaptation mechanism that estimates the unknown parameters [13]. The adaptation dynamics are based on immersive and invariance (I&I) ideas which allows to prove the state and parameter convergence with a relaxed excitation assumption [14].

This paper has been organized as follows: Section II presents the problem formulation with the nonlinear model and the OCV expression. In Section III, an observability analysis is presented. Section IV presents the high-gain observer designed. Section V introduces the parameter adaptation dynamics. All the study has been validated through numerical simulation in Section VI. Finally, Section VII presents the conclusions of the work.

## II. PROBLEM FORMULATION

A dynamic electrochemical model that has been widely used is the one proposed by Skyllas-Kazacos [15] that presents the evolution of the species concentration inside the cell and tanks. Using this approach, it has been formulated a nonlinear model for a VRFB that takes into account that the flow rates,  $q$ , and the total vanadium concentration,  $c_v$ , are different for the anolyte and catholyte. This nonlinear formulation can be expressed in terms of vanadium  $V^{2+}$  and  $V^{5+}$  species:

$$\begin{aligned} \dot{x}_1 &= \frac{2}{v_c} \left[ (x_3 - x_1)q_1 + \frac{I}{F} - k_2x_1 - k_4x_2 - 2k_5c_{v+} \right] \\ \dot{x}_2 &= \frac{2}{v_c} \left[ (x_4 - x_2)q_2 + \frac{I}{F} - k_3x_1 - k_5x_2 - k_c c_{v-} \right] \\ \dot{x}_3 &= \frac{1}{v_t} (x_1 - x_3)q_1 \\ \dot{x}_4 &= \frac{1}{v_t} (x_2 - x_4)q_2 \end{aligned} \quad (1)$$

where  $x_1$  is the concentration of  $V^{2+}$  in the anolyte cell,  $x_2$  is  $V^{5+}$  in the catholyte cell,  $x_3$  is the concentration of  $V^{2+}$  in the anolyte tank and  $x_4$  the ones of  $V^{2+}$  in the

catholyte tank.  $q_1$  is the flow rate in the anolyte and  $q_2$  in the catholyte,  $I$  is the charging or discharging current,  $F$  is the Faraday constant,  $k_i$  the diffusion coefficients of vanadium species  $i$ ,  $v_c$  is the volume of the cell and  $v_t$  the volume of each tank.

The expression of the cell voltage,  $E$ , considering the effect of the protons concentration inside the cell [16], as well as the ohmic losses is the following one:

$$E = E^\theta + \frac{RT}{F} \cdot \ln \left[ \left( \frac{x_2 \cdot (c_{H^+}(0) + x_2)^2}{c_{v-} - x_2} \right) \left( \frac{x_1}{c_{v+} - x_1} \right) \right] \pm rI \quad (2)$$

where  $E^\theta$  is the standard electrode potential,  $R$  is the gas constant,  $T$  is the cell temperature,  $c_{H^+}(0)$  is the initial proton concentration,  $c_{v+}$  is the total vanadium concentration in the catholyte part,  $c_{v-}$  in the anolyte, and  $r$  is the ohmic resistance considering the sign positive during a charging process and negative during the discharging one.

To compute the *SOC*, a distinction is made between the available Vanadium concentration in the catholyte and anolyte, generating two distinct *SOC* definitions,

$$SOC_- = \frac{x_3}{c_{v-}}, \quad SOC_+ = \frac{x_4}{c_{v+}}.$$

In this work, both definitions will be combined to present a unique *SOC* definition as follows:

$$SOC = \min\{SOC_-, SOC_+\}. \quad (3)$$

The objective is to design an observer that using the measured cell voltage can estimate the value of the states  $x_3$  and  $x_4$ , which is later used for the *SOC* estimation through (3).

To facilitate the design of the observer, and knowing that the current and temperature can be easily measured, it is possible to obtain a more simplified expression to work with. Assuming that  $E^\theta$  and  $r$  are constants, they can be subtracted from the cell voltage to obtain an expression  $h(x)$  that only depends on the cell concentrations  $x_1$ ,  $x_2$ ,  $c_{H^+}(0)$  and the total vanadium concentration  $c_{v-}$  and  $c_{v+}$

$$\begin{aligned} h(\mathbf{x}) &= \frac{E - E^\theta - \pm rI}{RT/F} \\ &= \ln \left[ \left( \frac{x_2 \cdot (c_{H^+}(0) + x_2)^2}{c_{v-} - x_2} \right) \left( \frac{x_1}{c_{v+} - x_1} \right) \right]. \end{aligned} \quad (4)$$

Taking into account this new expression, it is possible to formulate the nonlinear system with the following nomenclature:

$$\begin{aligned} \dot{\mathbf{x}} &= \mathbf{A}\mathbf{x} + q_1\mathbf{H}_1\mathbf{x} + q_2\mathbf{H}_2\mathbf{x} + \mathbf{c}I + \mathbf{d} \\ y &= h(\mathbf{x}) \end{aligned} \quad (5)$$

where  $\mathbf{x}$  are the concentrations, and matrices and vectors  $\mathbf{A}$ ,  $\mathbf{H}_1$ ,  $\mathbf{H}_2$ ,  $\mathbf{c}$  and  $\mathbf{d}$  have the following values:

$$\mathbf{A} = \frac{2}{v_c} \begin{bmatrix} -k_2 & -k_4 & 0 & 0 \\ -k_3 & -k_5 & 0 & 0 \\ 0 & 0 & 0 & 0 \\ 0 & 0 & 0 & 0 \end{bmatrix}$$

$$\mathbf{H}_1 = \begin{bmatrix} -\frac{2}{v_c} & 0 & \frac{2}{v_c} & 0 \\ 0 & 0 & 0 & 0 \\ \frac{1}{v_t} & 0 & -\frac{1}{v_t} & 0 \\ 0 & 0 & 0 & 0 \end{bmatrix} \quad \mathbf{H}_2 = \begin{bmatrix} 0 & 0 & 0 & 0 \\ 0 & -\frac{2}{v_c} & 0 & \frac{2}{v_c} \\ 0 & 0 & 0 & 0 \\ 0 & \frac{1}{v_t} & 0 & -\frac{1}{v_t} \end{bmatrix}$$

$$\mathbf{c} = \frac{2}{v_c} \begin{bmatrix} 1/F \\ 1/F \\ 0 \\ 0 \end{bmatrix} \quad \mathbf{d} = \frac{2}{v_c} \begin{bmatrix} -2k_5 c_{v+} \\ -k_c c_{v-} \\ 0 \\ 0 \end{bmatrix}.$$

### III. OBSERVABILITY ANALYSIS

First, it is crucial to study whether the states can be estimated from the model equations,  $\dot{x}$ , and the output  $y$ . A system is (locally) observable if it satisfies the observability rank condition, which implies that the rank of an observability space  $O_s$  must be equal to the number of states  $n$  [17]. For the concerned nonlinear system, the study of the observability rank condition can be done in a simple and automatic way computing the observability codistribution  $\Omega$ . For the case of study, the observability codistribution of order 4 is computed as follows [17]:

$$\Omega_4 = \text{span}\{\nabla h\} \oplus \text{span}\{\nabla L_{A_x+q_1 H_1 x+q_2 H_2 x} h(\mathbf{x})\} \\ \oplus \text{span}\{\nabla L_{A_x+q_1 H_1 x+q_2 H_2 x}^2 h\} \oplus \text{span}\{\nabla L_{A_x+q_1 H_1 x+q_2 H_2 x}^3 h\}$$

where  $\oplus$  is the direct sum operator, and  $L^i$  is the Lie derivative function that can be computed as:

$$L_{f(\mathbf{x})+g(\mathbf{x})}^1 h = \frac{\partial h}{\partial \mathbf{x}} \cdot (\mathbf{f}(\mathbf{x}) + g(\mathbf{x})) \\ L_{f(\mathbf{x})+g(\mathbf{x})}^k h = \frac{\partial L^{k-1} h}{\partial \mathbf{x}} \cdot (\mathbf{f}(\mathbf{x}) + g(\mathbf{x})).$$

Carrying out the analysis for the system formulated in (5) it can be shown that observability codistribution  $\Omega_4$  is full rank in the concerned operating region, therefore the system is observable and the concentrations can be recovered from the measured output.

### IV. OBSERVER DESIGN

Once the system observability has been analysed, the next step corresponds to the design of an appropriate observer capable of estimating the states  $x_3$  and  $x_4$ . The procedure to design the observer has been: first, transform the system to a strict feedback form, which accepts the design of a non-linear observer, and later, invert the transformation to recover the estimation in the original coordinates. In particular, consider following map:

$$\Phi(\mathbf{x}, q_1, q_2) \triangleq \begin{bmatrix} h(\mathbf{x}) \\ L_{A_x+q_1 H_1 x+q_2 H_2 x} h(\mathbf{x}) \\ \vdots \\ L_{A_x+q_1 H_1 x+q_2 H_2 x}^3 h(\mathbf{x}) \end{bmatrix}. \quad (6)$$

By means of the observability results in Section III, the map in (6) defines a diffeomorphism between the original variables in the concerned system and the new ones in the strict feedback form [18].

Consequently, it is possible to formulate a high-gain observer as follows [19]:

$$\dot{\hat{\mathbf{x}}} = \hat{\mathbf{A}}\hat{\mathbf{x}} + q_1 \mathbf{H}_1 \hat{\mathbf{x}} + q_2 \mathbf{H}_2 \hat{\mathbf{x}} + \mathbf{c}I + \mathbf{d} \\ + \left( \frac{\partial \Phi}{\partial \mathbf{x}} \right)^{-1} \left[ \frac{\alpha_1}{\epsilon}, \frac{\alpha_2}{\epsilon^2}, \frac{\alpha_3}{\epsilon^3}, \frac{\alpha_4}{\epsilon^4} \right]^\top (y - h(\hat{\mathbf{x}})) \quad (7)$$

where  $\alpha_i$  and  $\epsilon$  are the observer parameters to be designed and  $\hat{\mathbf{A}}$  is the matrix  $\mathbf{A}$  with the estimated values of the unknown parameters.

*Lemma 4.1:* [20] Consider the high-gain observer (7), and let the parameters  $\alpha_i$  be tuned such that the polynomial

$$s^4 + \alpha_1 s^4 + \alpha_2 s^3 + \alpha_3 s + \alpha_4 \quad (8)$$

has all the roots in the left half-plane. Then, there is a positive constant  $\epsilon^*$ , such that, for all  $\epsilon \leq \min\{\epsilon^*, 1\}$ , the estimation error of the observer (7) is ultimately bounded as follows

$$\|\mathbf{x} - \hat{\mathbf{x}}\| \leq \kappa_1 \|\mathbf{K} - \hat{\mathbf{K}}\|, \quad (9)$$

where  $\kappa_1$  are some positive constants and  $\mathbf{K} = \begin{bmatrix} k_2 \\ k_5 \end{bmatrix}$ .

*Remark 4.1:* To design the  $\epsilon$  it is important to take into account their properties. On the one hand, small values of  $\epsilon$  ensure fast convergence rates and observer robustness. On the other hand, too small values will induce the peaking phenomena and aggravate the observer noise sensitivity [20]. Taking into account these issues, It is important to correctly design the value of  $\epsilon$  to avoid these phenomena, while obtaining a correct estimate.

### V. PARAMETER ESTIMATION

In this work, it has been considered that only the diffusion rates  $k_2$  and  $k_5$  are unknown. Notice that these parameters appear in the first derivative of the concerned output function (4). Therefore, the unknown parameters appear on the considered observability map (6). Consequently, the observer will always present a bias that can not be reduced by means of increasing its gain.

This problem can be relaxed by means of a parameter estimation method based in I&I technique [14]. This approach is based on the design of an invariant and attractive manifold that can be used to estimate the parameters.

*Lemma 5.1:* Consider the following parameter estimation dynamics:

$$\dot{\hat{\theta}} = -\frac{\partial \beta(\hat{\mathbf{x}})}{\partial \mathbf{x}} \left[ f(\hat{\mathbf{x}}, \mathbf{u}) + \varphi(\hat{\mathbf{x}}) \left( \hat{\theta} + \beta(\hat{\mathbf{x}}) \right) \right] \\ \hat{\mathbf{K}} = \hat{\theta} + \beta(\hat{\mathbf{x}}), \quad (10)$$

where  $f(\hat{\mathbf{x}}, u)$ ,  $\varphi(\hat{\mathbf{x}})$  and  $\beta(\hat{\mathbf{x}})$  are the vector functions

$$f(\hat{\mathbf{x}}, \mathbf{u}) = \begin{bmatrix} \frac{2}{v_c} \left[ (\hat{x}_3 - \hat{x}_1)q_1 + \frac{I}{F} - k_4 \hat{x}_2 \right] \\ \frac{2}{v_c} \left[ (\hat{x}_4 - \hat{x}_2)q_2 + \frac{I}{F} - k_3 x_1 - k_c c_{v-} \right] \end{bmatrix}$$

$$\varphi(\hat{\mathbf{x}}) = \begin{bmatrix} -\hat{x}_1 & -2c_{v+} \\ 0 & -\hat{x}_2 \end{bmatrix} \quad \beta(\hat{\mathbf{x}}) = \frac{\gamma}{2} \begin{bmatrix} -\frac{1}{2}x_1^2 \\ -\frac{1}{2}x_2^2 \end{bmatrix} \quad (11)$$

been  $\gamma$  a positive constant to be tuned.

Then, the parameter estimation error will converge to:

$$\|\mathbf{K} - \hat{\mathbf{K}}\| \leq \kappa_2 \|\mathbf{x} - \hat{\mathbf{x}}\| \quad (12)$$

being  $\hat{\mathbf{K}} = \begin{bmatrix} \hat{k}_2 \\ \hat{k}_5 \end{bmatrix}$  and  $\kappa_2$  a positive constant.

*Proof:* Taking into account (11) the following expression can be obtained:

$$\frac{\partial \beta(\hat{\mathbf{x}})}{\partial \mathbf{x}} \varphi(\hat{\mathbf{x}}) = \gamma \begin{bmatrix} \frac{\hat{x}_1^2}{2} & \hat{x}_1 c_{v+} \\ 0 & \frac{\hat{x}_2^2}{2} \end{bmatrix},$$

that has positive eigenvalues. Then, define the following manifold  $\mathbf{z}$  as follows:

$$\mathbf{z} \triangleq \hat{\theta} - \mathbf{K} + \beta(\mathbf{x}). \quad (13)$$

The dynamics of the off-the-manifold coordinates  $\mathbf{z}$  are

$$\begin{aligned} \dot{\mathbf{z}} &= -\frac{\partial \beta(\mathbf{x})}{\partial \mathbf{x}} \varphi(\mathbf{x}) \mathbf{z} + \delta \\ &= -\gamma \begin{bmatrix} \frac{x_1^2}{2} & x_1 c_{v+} \\ 0 & \frac{x_2^2}{2} \end{bmatrix} \mathbf{z} + \delta \end{aligned} \quad (14)$$

where  $\delta$  is defined as:

$$\begin{aligned} \delta &\triangleq \frac{\partial \beta(\mathbf{x})}{\partial \mathbf{x}} \left[ f(\mathbf{x}, \mathbf{u}) + \varphi(\mathbf{x}) (\hat{\theta} + \beta(\mathbf{x})) \right] \\ &\quad - \frac{\partial \beta(\hat{\mathbf{x}})}{\partial \mathbf{x}} \left[ f(\hat{\mathbf{x}}, \mathbf{u}) + \varphi(\hat{\mathbf{x}}) (\hat{\theta} + \beta(\hat{\mathbf{x}})) \right]. \end{aligned} \quad (15)$$

As the functions  $\beta$ ,  $f(\mathbf{x}, \mathbf{u})$  and  $\varphi(\mathbf{x})$  are (locally) Lipschitz and the factor  $\frac{\partial \beta(\mathbf{x})}{\partial \mathbf{x}}$  is upper bounded, it is possible to find a positive constant  $L_\delta$  such that

$$\|\delta\| \leq L_\delta \|\mathbf{x} - \hat{\mathbf{x}}\|. \quad (16)$$

Now, consider the Lyapunov function candidate

$$V = \frac{1}{2} \mathbf{z}^\top \mathbf{z},$$

its derivative is

$$\dot{V} = -\gamma \mathbf{z}^\top \begin{bmatrix} \frac{x_1^2}{2} & x_1 c_{v+} \\ 0 & \frac{x_2^2}{2} \end{bmatrix} \mathbf{z} + \mathbf{z} \delta,$$

and considering the  $\delta$  bound expressed in (16) the following inequality is satisfied

$$\dot{V} \leq -\gamma \mathbf{z}^\top \begin{bmatrix} \frac{x_1^2}{2} & x_1 c_{v+} \\ 0 & \frac{x_2^2}{2} \end{bmatrix} \mathbf{z} + \mathbf{z} L_\delta \|\mathbf{x} - \hat{\mathbf{x}}\|. \quad (17)$$

TABLE I

VRFB SYSTEM PARAMETERS	
Variable	Value [units]
$v_c$	1 [ml]
$v_t$	45 [ml]
$c_{v-}$	0.35 [mol · l <sup>-1</sup> ]
$c_{v+}$	0.4 [mol · l <sup>-1</sup> ]
$c_{H^+}(0)$	1.6 [mol · l <sup>-1</sup> ]
$E^\theta$	1.267 [V]
$r$	1.33 [Ω]
$R$	8.311 [J · mol <sup>-1</sup> · K <sup>-1</sup> ]
$T$	297 [K]
$F$	96.485 [s · A · mol <sup>-1</sup> ]

As the matrix is not  $L_2$  integrable in all the operating region, it is possible to show that there is a positive constant  $\kappa_3$  such that the off-the-manifold variable is ultimately bounded as

$$\|\mathbf{z}\| \leq \kappa_3 \|\mathbf{x} - \hat{\mathbf{x}}\|. \quad (18)$$

Finally, by considering the parameter estimation (10), the off-the-manifold coordinate definition (13) and the fact that  $\beta(\mathbf{x})$  is Lipschitz, the bound (12) can be deduced. ■

#### A. Observer stability

It is important to properly select the conditions in which the coupling between the state observer and the parameter estimator remains stable.

It has been shown that the state-estimation error is input to the state stable taking the parameter-estimation error as an input, see (9). Moreover, a similar property is fulfilled for the parameter-estimation error, considering the state-estimation error as an input, see (12).

*Lemma 5.2:* The coupling between the high-gain observer (7) and the adaptation dynamics (10) is stable if the following holds:

$$\kappa_1 \kappa_2 \leq 1. \quad (19)$$

*Proof:* This statement can be proved by means of the small gain theorem [21]. ■

## VI. NUMERICAL SIMULATION

In order to validate the proposed *SOC* observer, a numerical simulation has been carried out. The parameters of the battery are summarized in Table I.

Regarding the current, it has been selected a charging process with a constant value of 1.8 A. For the case of the flow rates  $q_1$  and  $q_2$ , there has been considered as different, taking into account that in practice they will never be exactly the same. A flow rate of 100 ml/min has been considered in the catholyte part, and 110 ml/min in the anolyte.

Furthermore, the concentrations estimation have been initialized in a feasible point considering that the battery is practically discharged, presenting an initial 50% relative error<sup>1</sup>. As the diffusion coefficients are assumed to be unknown, their initial estimated values have been set to zero. In the true system, the values have been fixed to  $k_2 = 4.5 \cdot 10^{-11}$  and  $k_5 = 1.65 \cdot 10^{-11}$ .

Regarding the observer parameter tuning, the values of  $\alpha$  have been selected making Hurwitz the polynomial presented

<sup>1</sup>The relative error between  $x$  and  $\hat{x}$  is computed as:  $\frac{\|x - \hat{x}\|}{\|x\|} \cdot 100$

TABLE II  
VRFB SYSTEM PARAMETERS

Variable	Value
$\alpha_1$	$4 \cdot 10^{-4}$
$\alpha_2$	$5.81 \cdot 10^{-8}$
$\alpha_3$	$3.59 \cdot 10^{-12}$
$\alpha_4$	$7.8 \cdot 10^{-17}$
$\epsilon$	0.5
$\gamma$	$1 \cdot 10^{-7}$

in (8). For the case of the  $\epsilon$  constant, it has been designed to guarantee a balanced between perturbation rejection and noise sensitivity. On the other hand, for the diffusion coefficients estimator, the parameter  $\gamma$  has been adjusted to present an adequate parameter convergence rate while preserving the condition (19). All values of the observer design are summarized in Table II.

To analyze the robustness of the design relative to sensor noise, an 800 seconds simulation has been carried out introducing a high-frequency noise of variance 0.001 with respect to the voltage measurement, which is a reasonable value for a voltage sensor.

The simulations obtained show the correct operation of the coupling between the state observer and the parameter-estimation observer, obtaining a correct estimation in both *SOC* and the diffusion parameters. For the case of the *SOC*, which has been computed as the minimum between both catholyte and anolyte *SOC*'s, in Fig.2 it is shown how the error is reduced from a 43% presented in the initialization until a 0.0082% presented in the end of the simulation.

For the diffusion coefficient results, Fig.3 shows the estimation of the  $k_2$  and  $k_5$  coefficients, obtaining that there are correctly adjusted to the real ones. For the case of the  $k_2$  estimation, the error presented is 0.13%, while for the estimation of  $k_5$  its value does not exceed a 0.5%. In the detail, it can be observed how the  $k_5$  estimation presents a bias. This bias is due to the introduction of noise in the voltage output, which causes the estimation to not be perfectly estimated.

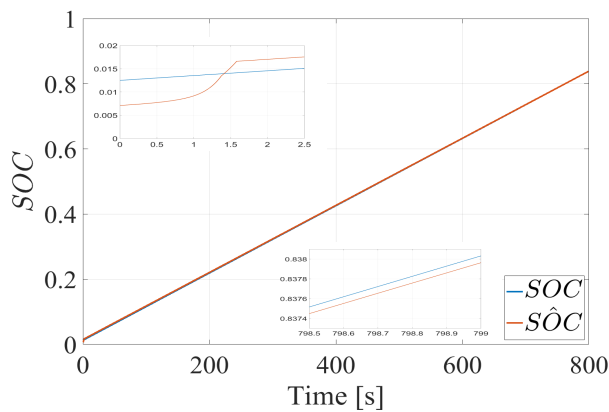


Fig. 2. Estimation of the *SOC* (red) versus the real value (blue).

## VII. CONCLUSIONS

This work has presented a non-linear observer to monitor correctly the states of a VRFB supposing differences, in

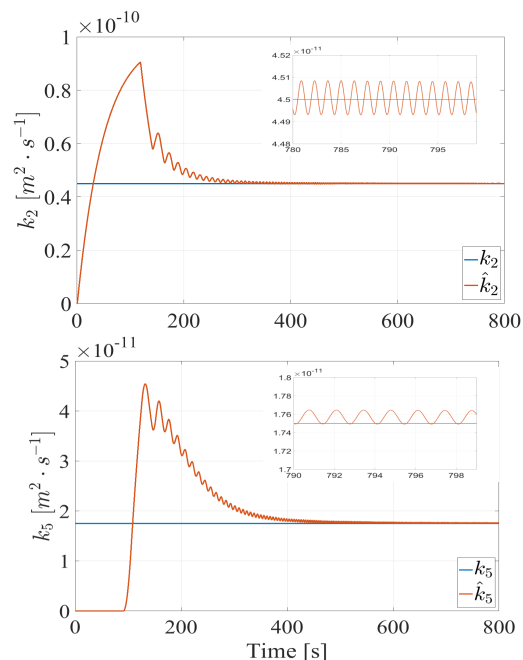


Fig. 3. Diffusion coefficients estimation (red) versus the real values (blue).  $k_2$  behaviour and detail (above) and  $k_5$  profile (below).

terms of flow rates and total vanadium species, between the catholyte and anolyte. For that reason, it has been possible to estimate separately both *SOC* presented in the system. Moreover, an online estimation of the diffusion parameters has been carried out using an *I&I* high-gain observer. The results have been validated in a numerical simulation where significant sensor noise is considered.

## REFERENCES

- [1] IEA. (2019) Renewables 2019-paris. [Online]. Available: <https://www.iea.org/reports/renewables-2019>
- [2] P. Alotto, M. Guarnieri, F. Moro, and A. Stella, "Redox flow batteries for large scale energy storage," in *2012 IEEE International Conference and Exhibition (ENERGYCON)*, 2012, pp. 293–298.
- [3] M. Guarnieri, P. Mattavelli, G. Petrone, and G. Spagnuolo, "Vanadium redox flow batteries: Potentials and challenges of an emerging storage technology," *IEEE Industrial Electronics Magazine*, vol. 10, no. 4, pp. 20–31, 2016.
- [4] A. Clemente, G. Ramos, and R. Costa-Castelló, "Voltage h $\infty$  control of a vanadium redox flow battery," *Electronics*, vol. 9, p. 1567, 09 2020.
- [5] A. Clemente and R. Costa-Castelló, "Redox flow batteries: A literature review oriented to automatic control," *Energies*, vol. 13, p. 4514, 09 2020.
- [6] M. Skyllas-Kazacos and M. Kazacos, "State of charge monitoring methods for vanadium redox flow battery control," *Journal of Power Sources*, vol. 196, no. 20, pp. 8822 – 8827, 2011.
- [7] B. Xiong, J. Zhao, Z. Wei, and M. Skyllas-Kazacos, "Extended kalman filter method for state of charge estimation of vanadium redox flow battery using thermal-dependent electrical model," *Journal of Power Sources*, vol. 262, pp. 50 – 61, 2014.
- [8] M. Mohamed, H. Ahmad, M. A. Seman, S. Razali, and M. Najib, "Electrical circuit model of a vanadium redox flow battery using extended kalman filter," *Journal of Power Sources*, vol. 239, pp. 284 – 293, 2013.
- [9] B. Xiong, J. Zhao, Z. Wei, and M. Skyllas-Kazacos, "Extended kalman filter method for state of charge estimation of vanadium redox flow battery using thermal-dependent electrical model," *Journal of Power Sources*, vol. 262, pp. 50 – 61, 2014.
- [10] B. Xiong, H. Zhang, X. Deng, and J. Tang, "State of charge estimation based on sliding mode observer for vanadium redox flow battery," in *2017 IEEE Power Energy Society General Meeting*, 2017, pp. 1–5.

- [11] Z. Wei, K. J. Tseng, N. Wai, T. M. Lim, and M. Skyllas-Kazacos, "Adaptive estimation of state of charge and capacity with online identified battery model for vanadium redox flow battery," *Journal of Power Sources*, vol. 332, pp. 389 – 398, 2016.
- [12] A. Cecilia and R. Costa-Castelló, "Observador de alta ganancia con zona muerta ajustable para estimar la saturación de agua líquida en pilas de combustible tipo pem," *Revista Iberoamericana de Automática e Informática industrial*, vol. 17, no. 2, pp. 169–180, 2020.
- [13] A. Cecilia, M. Serra, and R. Costa-Castelló, "Pemfc state and parameter estimation through a high-gain based adaptive observer," *21st IFAC World Congress*, 07 2020.
- [14] A. Astolfi and R. Ortega, "Immersion and invariance: a new tool for stabilization and adaptive control of nonlinear systems," *IEEE Transactions on Automatic Control*, vol. 48, no. 4, pp. 590–606, 2003.
- [15] Z. Wei, R. Xiong, T. M. Lim, S. Meng, and M. Skyllas-Kazacos, "Online monitoring of state of charge and capacity loss for vanadium redox flow battery based on autoregressive exogenous modeling," *Journal of Power Sources*, vol. 402, pp. 252 – 262, 2018.
- [16] K. Knehr and E. Kumbur, "Open circuit voltage of vanadium redox flow batteries: Discrepancy between models and experiments," *Electrochemistry Communications*, vol. 13, no. 4, pp. 342 – 345, 2011.
- [17] G. Besançon, *Nonlinear observers and applications*. Springer, 2007, vol. 363.
- [18] P. Bernard, L. Praly, V. Andrieu, and H. Hammouri, "On the triangular canonical form for uniformly observable controlled systems," *Automatica*, vol. 85, pp. 293 – 300, 2017.
- [19] D. Astolfi and L. Praly, "Output feedback stabilization for siso nonlinear systems with an observer in the original coordinates," in *52nd IEEE Conference on Decision and Control*, 2013, pp. 5927–5932.
- [20] H. K. Khalil and L. Praly, "High-gain observers in nonlinear feedback control," *International Journal of Robust and Nonlinear Control*, vol. 24, no. 6, pp. 993–1015, 2014.
- [21] Z.-P. Jiang, A. R. Teel, and L. Praly, "Small-gain theorem for iss systems and applications," *Mathematics of Control, Signals and Systems*, vol. 7, no. 2, pp. 95–120, 1994.